Measurement of Calcium Channel Inactivation Is Dependent upon the Test Pulse Potential

Shalini Gera and Lou Byerly
Department of Biological Sciences, University of Southern California, Los Angeles, California 90089-2520 USA

ABSTRACT We have developed two methods to measure Ca^{2+} channel inactivation in *Lymnaea* neurons—one method, based upon the conventional double-pulse protocol, uses currents during a moderately large depolarizing pulse, and the other uses tail currents after a very strong activating pulse. Both methods avoid contamination by proton currents and are unaffected by rundown of Ca^{2+} current. The magnitude of inactivation measured differs for the two methods; this difference arises because the measurement of inactivation is inherently dependent upon the test pulse voltage used to monitor the Ca^{2+} channel conductance. We discuss two models that can generate such test pulse dependence of inactivation measurements—a two-channel model and a two-open-state model. The first model accounts for this by assuming the existence of two types of Ca^{2+} channels, different proportions of which are activated by the different test pulses. The second model assumes only one Ca^{2+} channel type, with two closed and open states; in this model, the test pulse dependence is due to the differential activation of channels in the two closed states by the test pulses. Test pulse dependence of inactivation measurements of Ca^{2+} channels may be a general phenomenon that has been overlooked in previous studies.

INTRODUCTION

Ca^{2+} channel inactivation is often measured as the decay of Ca^{2+} current during a prolonged depolarization. However, this method of measuring inactivation can only be applied at potentials that elicit an appreciable Ca^{2+} current. A common alternative to this method is the double-pulse protocol, in which a conditioning pulse is followed by a pulse to a fixed voltage (a test pulse); this test pulse reveals the number of channels that are capable of being activated. In this case, inactivation caused by the conditioning pulse is measured as the percentage reduction in the test pulse current when a conditioning pulse precedes the test pulse. The test pulse is usually chosen so that it elicits maximum Ca^{2+} current, and it is generally assumed that the measurement of inactivation is independent of the test pulse potential. We have developed another method of measuring inactivation that enables us to use a broad range of test pulse potentials. We were surprised to find that inactivation measurements vary significantly with the test pulse potential.

The experiments presented in this study were performed on native molluscan Ca^{2+} channels. Studies of native Ca^{2+} channels do have problems of contaminating currents and of lack of molecular definition of Ca^{2+} channels, problems that are largely avoided by studies of heterologously expressed Ca^{2+} channels. However, there is considerable evidence to suggest that Ca^{2+} channel inactivation depends upon the intracellular environment (Tillotson, 1979; Isom et al., 1994; Johnson and Byerly, 1994; Olcese et al., 1994; Schuhmann et al., 1997), and important components of the neuronal intracellular environment may be missing from heterologous expression systems. Studies of Ca^{2+} channels in their native environment are, therefore, essential for studying physiologically relevant Ca^{2+} channel inactivation.

Inactivation of Ca^{2+} channels is thought to have two components: a voltage-dependent component and a Ca^{2+}-dependent component. Many of the earliest studies on Ca^{2+} channel inactivation used molluscan neurons, and these established the presence of a large Ca^{2+}-dependent component of inactivation in these neurons (Tillotson, 1979; Eckert and Tillotson, 1981). However, these early studies did not take into account the outward proton current, which was discovered later in molluscan neurons (Thomas and Meech, 1982; Byerly et al., 1984) and often contributes to the appearance of Ca^{2+} current inactivation.

In this study we use two methods to study voltage-dependent inactivation of Ca^{2+} channels in neurons of the freshwater snail *Lymnaea stagnalis*. The Ca^{2+}-dependent component of inactivation has been suppressed by strongly buffering the intracellular Ca^{2+} to low levels (Gera and Byerly, 1998). The first method of measuring inactivation is based upon the more conventional double-pulse protocol, and the second method takes advantage of the fast voltage-clamping techniques currently available and uses tail currents to measure the inactivation of Ca^{2+} channels. Both methods avoid contamination by H^+ currents and are insensitive to rundown. The measurements of inactivation made with the two methods differ systematically over a large range of voltages; this difference arises from the different test pulse voltages used by the two methods. We describe two models that can generate the test pulse dependence of inactivation measurements. Both models account for this behavior by assuming that Ca^{2+} channels are dis-

Received for publication 13 August 1998 and in final form 16 March 1999.
Address reprint requests to Dr. Shalini Gera, Beckman Center B177, Molecular and Cellular Physiology Department, Stanford University School of Medicine, Stanford, CA 94305-5426. Tel.: 650-723-7557; Fax: 650-725-4463; E-mail: sgera@cmgm.stanford.edu.

0006-3495/99/06/3076/13 $2.00

tributed into distinct classes or closed states, different proportions of which are activated by different test pulses.

MATERIALS AND METHODS

Cell preparation and electrophysiology

Neurons from the pedal, parietal, and visceral ganglia of adult *Lymnaea stagnalis,* a freshwater snail, were prepared for patch clamp experiments as previously described (Johnson and Byerly, 1993). Briefly, the ganglia are treated with enzymes (Sigma P5147, Protease Type XIV, 1 mg/ml for 20 min, and Sigma T8918, trypsin, 2 mg/ml for 1 h at 29°C) and subsequently desheathed. The neurons in the ganglia are mechanically dissociated and stored in a glucose-containing *Lymnaea* saline. These cells have normal currents for 20 h after dissociation if stored in a refrigerator. Nearly spherical cells with diameters ranging from 50 to 75 μm were used for this study.

Currents were recorded using the Axopatch 200A patch clamp amplifier. pClamp software (version 6.0) was used for data acquisition (Clampex) and analysis (Clampfit). Patch clamp electrodes were pulled in two steps from VWR micropipettes, using a Narashige PP-83 electrode puller, and then coated with Sylgard (Dow Corning) to reduce electrode capacitance. These electrodes typically had resistances of 1 MΩ and tip diameters of 12–16 μm. Series resistance (usually around 2–4 MΩ) was electronically compensated to more than 90%. Inactivation measurements were taken at least 10 min after the whole cell configuration was entered, to allow for the diffusion of the electrode solution into the cell. Junction potential errors (described in Hagiwara and Ohmori, 1982; Neher, 1995) have not been corrected for in these experiments and are expected to be approximately -10 to -15 mV (Byerly and Hagiwara, 1982).

Linear leak currents and capacitive transients are subtracted using a P/4 protocol. All voltage-gated Na^+ and K^+ currents are eliminated by using Cs^+ and $Tris^+$ as the major cations in the standard intracellular and extracellular solutions, respectively (see Solutions). Currents recorded in the standard solutions comprise voltage-gated Ca^{2+} and H^+ currents (Byerly et al., 1984). These currents are not contaminated with outward Cs^+ or Cl^- currents, because replacing internal Cs^+ with *N*-methyl-D-glucamine$^+$ or external Cl^- with methanesulfonate$^-$ ($CH_3SO_3^-$) does not produce any change in the shape of the recorded currents.

Solutions

The *Lymnaea* saline used for dissociation and storage of cells contains 50 mM NaCl, 2.5 mM KCl, 4 mM $MgCl_2$, 4 mM $CaCl_2$, and 10 mM HEPES, adjusted to pH 7.4 with NaOH. The standard extracellular saline used for recording Ca^{2+} or Ba^{2+} currents is composed of 76 mM TrisCl and 10 mM $CaCl_2$ or $BaCl_2$ adjusted to pH 7.4. The intracellular solution contains 50 mM HEPES, 0.5 mM $MgCl_2$, 3–12 mM CsCl, 15–20 mM aspartic acid, 2 mM Mg-ATP, and 5 mM EGTA, adjusted to pH 7.3 with CsOH.

Measurement of tail currents

The tail currents were measured using a four-pole Bessel filter with a cutoff frequency of 10 kHz, and the currents were digitized at 100 kHz. Reducing the cutoff frequency to 5 kHz did slow slightly the time course of the tail currents but did not change the inactivation measurements. The clearest indication of the speed of the voltage clamp obtained was provided by the rise time of the tail currents. Tail currents typically reached their peak magnitude in 100 μs, independently of the magnitude of the current. Although the finite speed of the clamp reduces the magnitude of the measured tail currents, we are convinced that these tail currents are a reliable measure of the Ca^{2+} conductance that exists just before the negative step in potential. These tail currents indicate that the Ca channels activate with the expected Boltzmann-shaped voltage dependence (Fig. 7 *A*). Furthermore, if the limited speed of the clamp were truncating large tail currents more than small ones, we would expect cells with larger tail currents to show smaller amounts of measured inactivation—however, no correlation between inactivation measurements and tail current magnitudes was found.

Large gating currents, unsubtracted leak currents, or currents due to other conductances (such as H^+ currents, Byerly et al., 1984) can also contaminate tail currents, making them an unsuitable measure of Ca^{2+} channel conductance. However, we have determined that these extraneous components, if present in our Ca^{2+} tail current measurements, are negligible. When the Ba^{2+} ion concentration in the extracellular saline is reduced from 10 to 3 mM and to 0.5 mM, the tail currents, after a pulse to $+120$ mV, decline in magnitude, as do the pulse currents, and both approach zero as the Ba^{2+} concentration does (Fig. 1 *A*). This supports the conclusion that peak tail currents (and pulse currents) are entirely due to

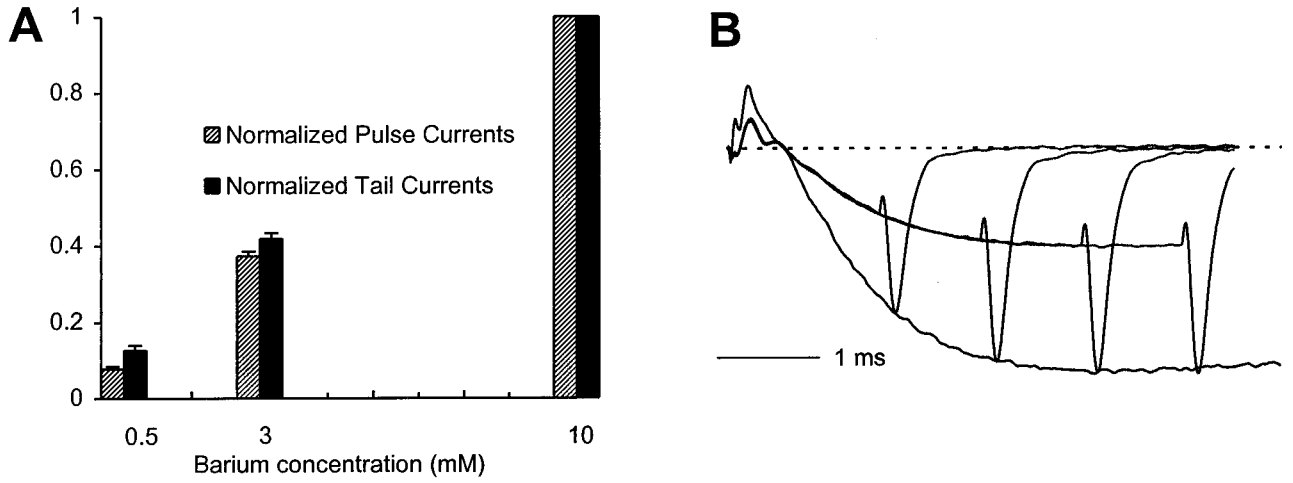

FIGURE 1 Tail currents are carried by ions flowing through Ca^{2+} channels. (*A*) Pulse currents and tail currents are reduced in proportion as extracellular Ba^{2+} concentration is reduced from 10 to 3 mM ($n = 9$) and to 0.5 mM ($n = 5$). Tail currents after a pulse to $+120$ mV are measured at -20 mV. Tail currents and peak inward pulse currents are normalized to their values in 10 mM Ba^{2+}. In these experiments external Ba^{2+} was replaced by external Mg^{2+} to keep the external divalent concentration at 10 mM. It was not possible to do these experiments when all permeant divalents were replaced by Mg^{2+}, because this caused the cells to become leaky. Error bars in this and following figures represent SEM. (*B*) Tail currents after a depolarization to $+30$ mV of variable duration and pulse current at $+30$ mV reflect the same kinetics of Ca^{2+} channel activation. The lowest trace is a longer pulse current to $+30$ mV, normalized to the amplitude of the tail currents.

ions flowing through Ca^{2+} channels, in this case Ba^{2+} ions. Furthermore, tail currents measured at different times during a step to +30 mV show the same time course of current activation as the pulse current (Fig. 1 *B*). For a small voltage step such as this, the pulse current is a reliable measure of Ca^{2+} channel activation, because the H^+ conductance is very small at these voltages. The agreement between pulse and tail currents in these cases indicates that our measurements of Ca^{2+} tail currents are relatively free of contamination and adequately reflect the Ca^{2+} channel conductance.

Protocols for measuring inactivation

The two methods for measuring inactivation are described in detail in the Results (Fig. 2). We standardly use 150-ms-long conditioning pulses in these protocols because longer pulses cause a faster rundown of Ca^{2+} current. The conditioning pulse is followed by a 20-ms gap before the currents are activated again to measure inactivation. In method 1, the membrane is held at −60 mV for the entire 20-ms duration of the gap, whereas in method 2, the membrane is held at −60 mV for the first 17.5 ms and then is stepped to +120 mV for the remaining 2.5 ms. This is done so that the peak pulse current in method 1 and peak tail current in method 2 are measured at approximately the same time after the conditioning pulse. This gap is necessary to completely deactivate H^+ and Ca^{2+} channels. Ideally, this gap should be minimal, so that the channels that have inactivated during the conditioning pulse are not allowed time to recover from inactivation. However, the slow tail currents elicited by strong depolarizations during the conditioning pulse can take up to 20 ms to turn off, which limits how short the gap duration can be.

The two different protocols used in methods 1 and 2 would be expected to yield slight differences in measurement of inactivation. One reason for this is that the reference pulse used in method 1 may itself cause some inactivation from which the channels do not completely recover by the time the test pulse current is measured 170 ms later. Therefore, inactivation measured by method 1 measures the residual inactivation caused by the reference pulse in addition to the inactivation due to the conditioning pulse. Method 2, on the other hand, uses no reference pulse. The second possible source of difference is that in method 1, the inactivated channels recover from inactivation at −60 mV for 20 ms during the gap, whereas in method 2, they recover at −60 mV for 17.5 ms and at +120 mV for 2.5 ms, where recovery is probably different. However, these differences are very small and can be neglected in most cases. This is demonstrated for lower test potentials by experiments in which methods 1 and 2 are modified so that both use a test pulse of +30 mV, and the resulting measurements of inactivation are quite similar for all conditioning pulse voltages (see Fig. 4 *C*).

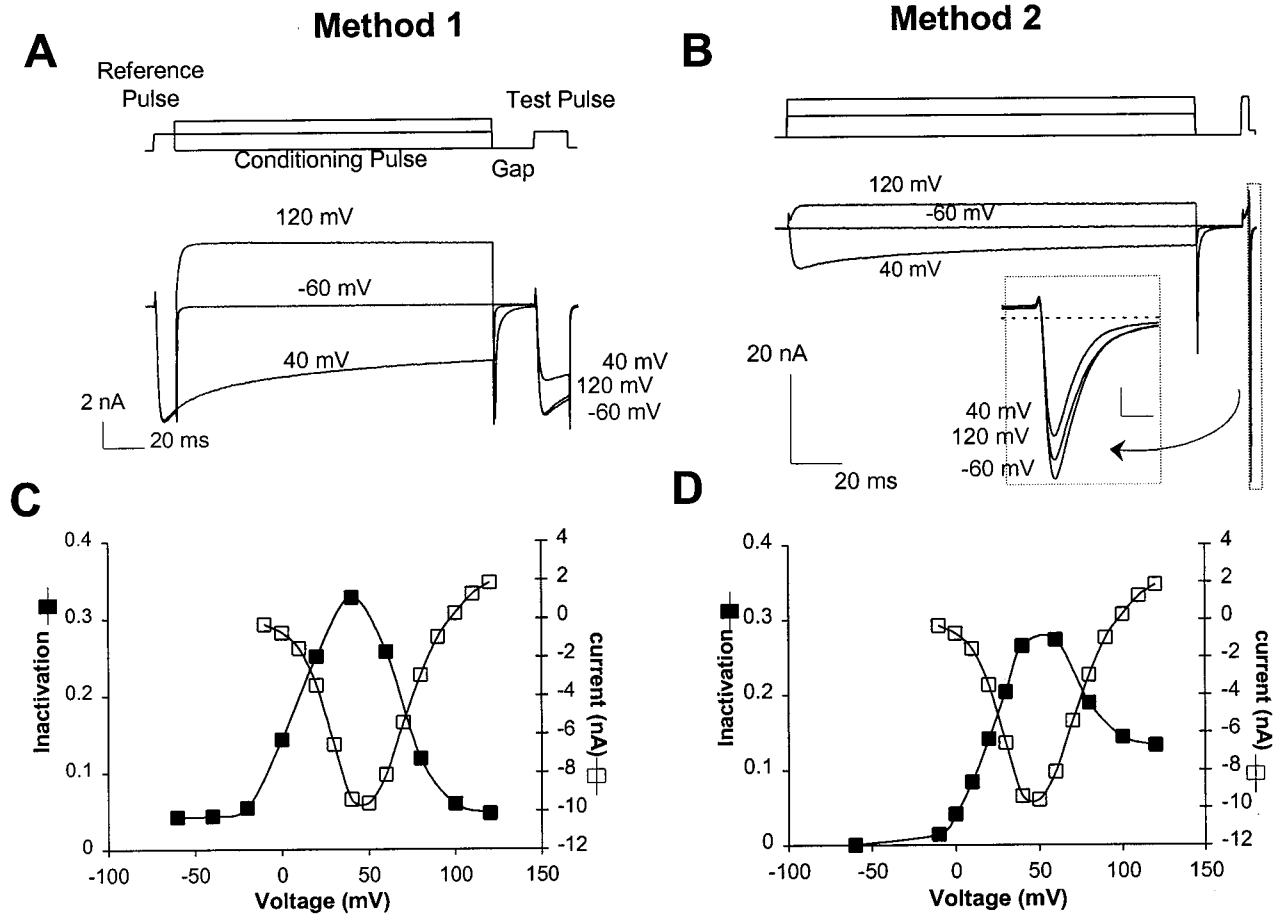

FIGURE 2 Methods of measuring Ca^{2+} channel inactivation. (*A*) Method 1 command voltage traces for three different conditioning pulse voltages (*above*) and the corresponding current traces (*below*). Method 1 uses a 10-ms reference pulse to +40 mV and a 150-ms conditioning pulse, followed by a 20-ms gap at the holding potential (−60 mV) and a test pulse to +40 mV. (*B*) Method 2 command voltage and current traces from the cell in *A*. In this method, after the 150-ms conditioning pulse, there is a 17.5-ms gap at −60 mV and a 2.5-ms test pulse to +120 mV. The tail currents at the end of the test pulse are measured at −40 mV and are shown in the inset for clarity (the scale bars represent 10 nA and 2.5 ms). (*C* and *D*) Inactivation (■) measured using method 1 or method 2, respectively, as a function of the conditioning pulse voltage, and the peak inward current measured at each voltage (□) for the cell in *A* and *B*.

Measurements of inactivation are insensitive to rundown

Rundown of Ca^{2+} currents can interfere with measurements of inactivation, because it also causes a decrease in the overall Ca^{2+} current magnitude, although on a slower time scale (typically, the Ca^{2+} current takes 10 min to run down by 10% during an experiment). If the reference pulse and the test pulse are separated by a large enough period of time, then the decline in current measured by the test pulse may be due to both rundown and inactivation. Both methods 1 and 2 avoid this problem, but in different ways. In method 1, the test pulse follows the reference pulse after 170 ms, which is too short an interval to allow rundown. In method 2, the same strategy cannot be used to avoid rundown because of technical reasons (the tail currents are measured at a faster digitization rate; however, our aquisition software does not allow the use of more than two digitization rates during the same episode). Thus, in method 2, the reference tail current is measured once for every two test tail currents, and the longest period between a reference tail current measurement and a test tail current measurement is 20 s. During this period the reference tail current changes by less than 1% on average. It is also possible that rundown over a period of time may change the inactivation properties of the Ca^{2+} current itself. However, we find that under our experimental conditions, rundown of Ca^{2+} current is not accompanied by any change in the inactivation curve. We have consistently observed that even in cases where the Ca^{2+} current rundown was extreme (more than 50% of its original value), the inactivation curves measured using the same method change by less than 10%.

RESULTS

Two methods for measuring Ca^{2+} channel inactivation

Ca^{2+} channel inactivation is commonly measured using a double-pulse protocol. A variant of this protocol is used in this study and is illustrated in Fig. 2 *A*. In this method (henceforth referred to as method 1), three voltage pulses are applied—a short "reference pulse" to +40 mV, a 150-ms "conditioning pulse" of variable amplitude, and a "test pulse," also to +40 mV. A 20-ms "gap" separates the test pulse from the conditioning pulse. If no inactivation occurs during the conditioning pulse, then the test pulse current is identical to the reference pulse current. When Ca^{2+} channels inactivate during the conditioning pulse, the test pulse current is reduced relative to the reference pulse current. Inactivation, for any conditioning pulse voltage, is calculated using the following expression:

$$\text{Inactivation} = \frac{I_{rp} - I_{tp}}{I_{rp}},$$

where I_{rp} and I_{tp} refer to the peak inward currents measured during the reference and test pulses, preceding and following the conditioning pulse.

Although this method is advantageous in that it is simple to use, it is not reliable when the Ca^{2+} current is very small (such as at very positive test potentials) or when an outward current contaminates the Ca^{2+} current. To measure inactivation under these conditions, we have developed a new protocol, method 2, which uses tail currents to measure inactivation and is described below. Ca^{2+} channel tail currents can be reliably measured, even when the Ca^{2+} pulse currents (i.e., currents during an activating voltage step) are small, and are easier to isolate from other currents not flowing through Ca^{2+} channels.

Method 2 (Fig. 2 *B*) is similar to method 1, except that it uses tail currents (after a short activating pulse to +120 mV) to monitor the Ca^{2+} conductance of the cell, instead of pulse currents during a test pulse to +40 mV. The 150-ms conditioning pulse is followed by a gap, as in method 1, and then a brief test pulse to +120 mV is applied. The pulse is ended by a step to −40 mV, which elicits a large Ca^{2+} tail current, and this is taken as a measure of the Ca^{2+} conductance of the cell. The tail current measured at the end of a test pulse after a conditioning pulse to −60 mV (the holding potential) is taken as the "reference tail current." Ca^{2+} channel inactivation during a conditioning pulse causes a reduction in the corresponding tail current, compared to the reference tail current. Inactivation caused by a conditioning pulse voltage, in this method, is calculated as follows:

$$\text{Inactivation} = \frac{I_{rt} - I_{tt}}{I_{rt}},$$

where I_{rt} is the reference tail current and I_{tt} is the tail current after the test pulse to +120 mV after the conditioning pulse. To minimize the effect of time-dependent changes in Ca^{2+} current (due to rundown or changes in series resistance), one reference tail current measurement is taken for every set of two conditioning pulses to nonreference voltages. In both methods, the voltage protocols are applied 10 s apart.

Methods 1 and 2 give different measurements of inactivation

Both methods of measuring inactivation yield bell-shaped inactivation curves with maximum inactivation for conditioning pulse voltages of +40 to +60 mV (Fig. 2, *C* and *D*). Note, however, that although the two methods in Fig. 2 are applied to the same cell under identical conditions, they do not give identical inactivation curves. We find that there is a consistent difference between the two measures of inactivation for most conditioning pulse voltages, irrespective of the order in which the measurements are taken. For lower conditioning pulse voltages ($\leq$60 mV), inactivation measured by method 1 is greater than that measured by method 2; whereas for higher conditioning pulse voltages ($\geq$60 mV), method 2 measurements of inactivation are larger than method 1 measurements (Fig. 3 *A*). The two measurements are strongly correlated in all cells studied (Fig. 3 *B*), and the differences between them are very reproducible. These differences, therefore, are not due to random errors in measurement, or other factors that are independent of Ca^{2+} current inactivation.

Measurements of inactivation depend upon test pulse potentials

The discrepancies between the measurements of inactivation obtained using the two methods can be explained by the

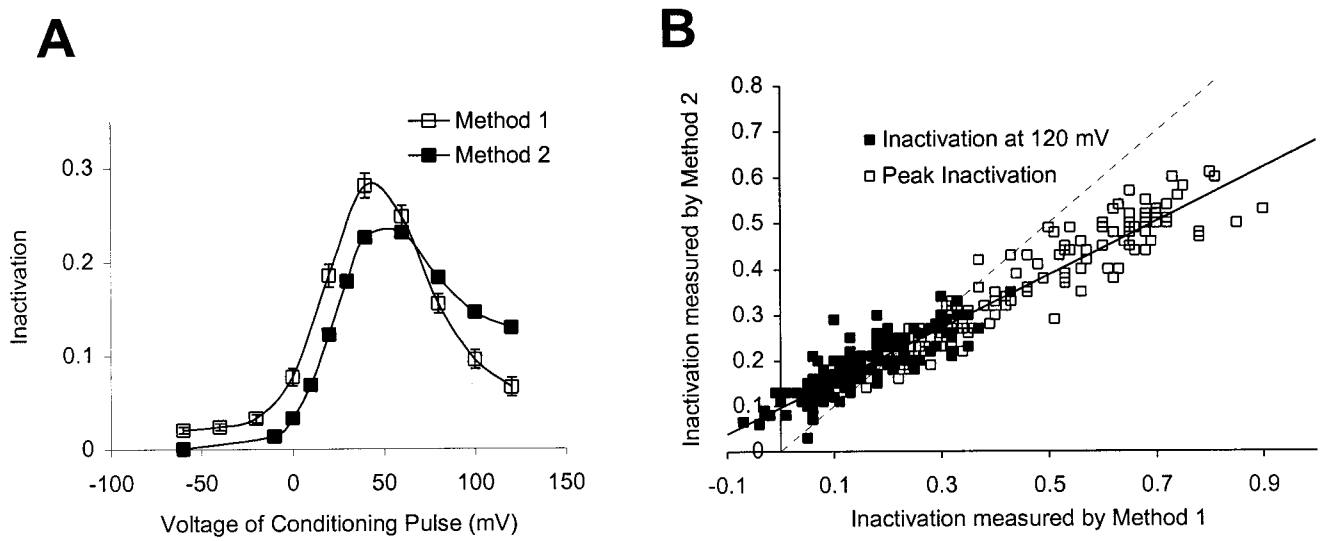

FIGURE 3 Comparison of inactivation measured by methods 1 and 2. (*A*) Average inactivation curves using methods 1 (□, $n = 34$) and 2 (■, $n = 54$). Error bars indicate SEM, but in some cases they are too small to be seen distinctly from the marker. (*B*) Linear relation between inactivation measured by methods 1 and 2 in individual cells. Open symbols (□) represent measurements of peak inactivation, and closed symbols (■) represent inactivation measured for conditioning pulses to +120 mV. Data shown here are taken from 172 cells in which inactivation was measured under a number of different conditions (e.g., different concentrations of internal Ca^{2+} buffers, substitution of external Ca^{2+} with Ba^{2+}, partial block of Ca^{2+} current with Co^{2+}). The data are fitted by a line with slope 0.58 and a *y*-intercept of 0.1 ($R^2 = 0.91$). The dashed line has a slope of unity and is shown for comparison.

sensitivity of both methods to the test pulse voltage. The two methods use different test pulse voltages—the test pulse in method 1 is to +40 mV, whereas that in method 2 is to +120 mV—and the measurement of inactivation in both methods depends upon the test pulse potential used. As the test pulse voltage in method 2 is decreased from +120 mV to +30 mV, the peak inactivation increases while the inactivation for pulses to +120 mV decreases (Fig. 4 *A*). A similar trend is also seen when the test pulse voltage in method 1 is decreased from +30 mV to +20 mV (Fig. 4 *B*). Therefore, the main reason for the difference between measurements of inactivation using the two methods is that method 1 uses a test pulse to +40 mV to measure the state of Ca^{2+} channels, whereas method 2 uses a test pulse to +120 mV. Indeed, when the test pulse is to +30 mV for both protocols (Fig. 4 *C*), the inactivation measured using method 1 is in good agreement with that determined with method 2; the slight difference in the measurements here is expected because of some residual inactivation produced by the initial reference pulse in method 1 and is of a nature different from that seen in Fig. 4 *A*.

We do not know what causes the measurements of inactivation to be sensitive to test pulse voltage. We have examined the possibility that H^+ currents may be contaminating the inactivation measurements in one or both methods and thus making the measurements sensitive to the test pulse potential. We have also investigated whether the slow tail currents following large positive pulses may cause error in measurements of Ca^{2+} current during or after the test pulse. However, we show below that neither of these two possibilities can explain the discrepancy between the inactivation measurements resulting from the two methods and their dependence upon the test pulse potentials. Because it is only by using tail current magnitudes that we can measure inactivation over a large range of test potentials, we have also conducted control experiments to ensure that our tail current measurements accurately reflect Ca^{2+} channel conductance (see Materials and Methods). This leads us to believe that the test pulse dependence of inactivation described above is not due to erroneous measurements of inactivation for some test pulse potentials, but it is an inherent property of the Ca^{2+} current in *Lymnaea* channels.

It is possible to model the test pulse dependence of the measurement of inactivation by assuming a heterogeneous population of Ca^{2+} channels with different activation and inactivation properties. Alternatively, this test pulse dependence of inactivation measurement can also be modeled by assuming only one class of channels with two open and two closed states, with one of the open states leading to an inactivated state. Both of these models are developed in the Discussion.

Measurements of inactivation are independent of H^+ current

Many molluscan neurons have an outward H^+ current that cannot be readily isolated from the Ca^{2+} current, as no pharmacological agent selectively blocks it (Thomas and Meech, 1982). *Lymnaea* neuron currents recorded in our Ca^{2+} current recording solutions consist of Ca^{2+} and H^+ currents (Byerly et al., 1984). Addition of 10 mM tetrapentylammonium (TPeA) to the external solution blocks all but H^+ currents and is used for isolating H^+ currents (Johnson

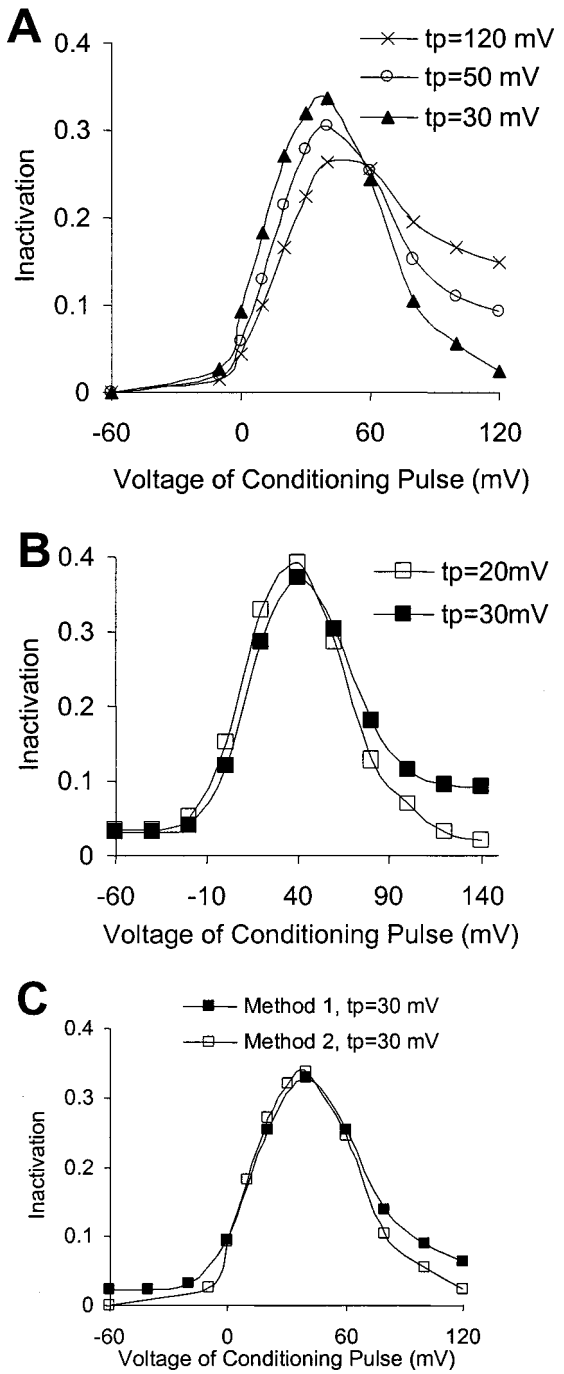

FIGURE 4 The difference between measurements of inactivation by methods 1 and 2 is due to the different test pulse potentials used. (*A*) Inactivation was measured in the same cells ($n = 4$) by Method 2 with the test pulse to +30 mV (▲), +50 mV (○), and +120 mV (×). (*B*) Inactivation curves obtained in the same cells ($n = 9$), using method 1 with the test pulse potential to +20 mV (□) and to +30 mV (■). (*C*) Inactivation measured using the same test pulse potential of 30 mV in method 1 (■) and in method 2 (□) gives similar inactivation curves ($n = 4$). Symbols represent mean values.

and Byerly, 1993). Subtraction of H^+ current from the current recorded in the standard external solutions gives a measurement of the Ca^{2+} current alone (Fig. 5 *A*). Currents measured in TPeA show that in *Lymnaea* neurons at physiological extra- and intracellular pH, H^+ current activates at potentials above +40 mV and can have magnitudes comparable to that of Ca^{2+} channel current. However, TPeA usually caused the cells to develop a large leak current and, hence, was not used regularly to isolate H^+ currents in this study.

H^+ currents and method 1

One possible source of error in using method 1 to measure inactivation is contamination of test and reference pulse currents by H^+ currents. It is for this reason that we choose the reference and test pulse potential in method 1 to be +40 mV; at this voltage there is a large inward Ca^{2+} current, but only a very small and slowly activating H^+ current, allowing for a relatively pure peak Ca^{2+} current measurement. Note, however, that the Ca^{2+} current used by reference and test pulses is not the maximum Ca^{2+} current, which occurs for more positive voltages. Any H^+ current activated during the conditioning pulse is given time to completely deactivate during the 20-ms gap at −60 mV after the conditioning pulse (Byerly et al., 1984), so that test pulse current is not contaminated by H^+ current.

It is illustrative to consider what the effect on inactivation measurement would be if H^+ currents were present in the reference and test pulse currents. In that case, cells with outward H^+ currents would appear to have smaller inward reference and test pulse currents. The conditioning pulse does not affect the proton current during the pulse (I^H), and therefore the measured inactivation would be given by the following:

$$\text{Measured Inactivation}$$

$$= \frac{(I_{rp}^{Ca} - I^H) - (I_{tp}^{Ca} - I^H)}{(I_{rp}^{Ca} - I^H)} = \frac{I_{rp}^{Ca} - I_{tp}^{Ca}}{I_{rp}^{Ca} - I^H}$$

$$\geq \frac{I_{rp}^{Ca} - I_{tp}^{Ca}}{I_{rp}^{Ca}} = \text{Actual Inactivation}$$

(Here, all I's represent current magnitudes and are positive numbers.)

Hence, inactivation measured using method 1 would be larger than actual, if the H^+ currents were contaminating our measurements of peak Ca^{2+} currents. Moreover, in this case, cells with larger H^+ currents would appear to have larger values of inactivation; however, we do not see such a relationship. Peak measurements of inactivation measured using method 1 are completely unrelated to H^+ current magnitude (Fig. 5 *B*); therefore, we conclude that the measurement of inactivation using method 1 is insensitive to H^+ currents.

H^+ currents and method 2

In method 2, the test pulse is to +120 mV, and it activates a substantial outward current, most of which is believed to

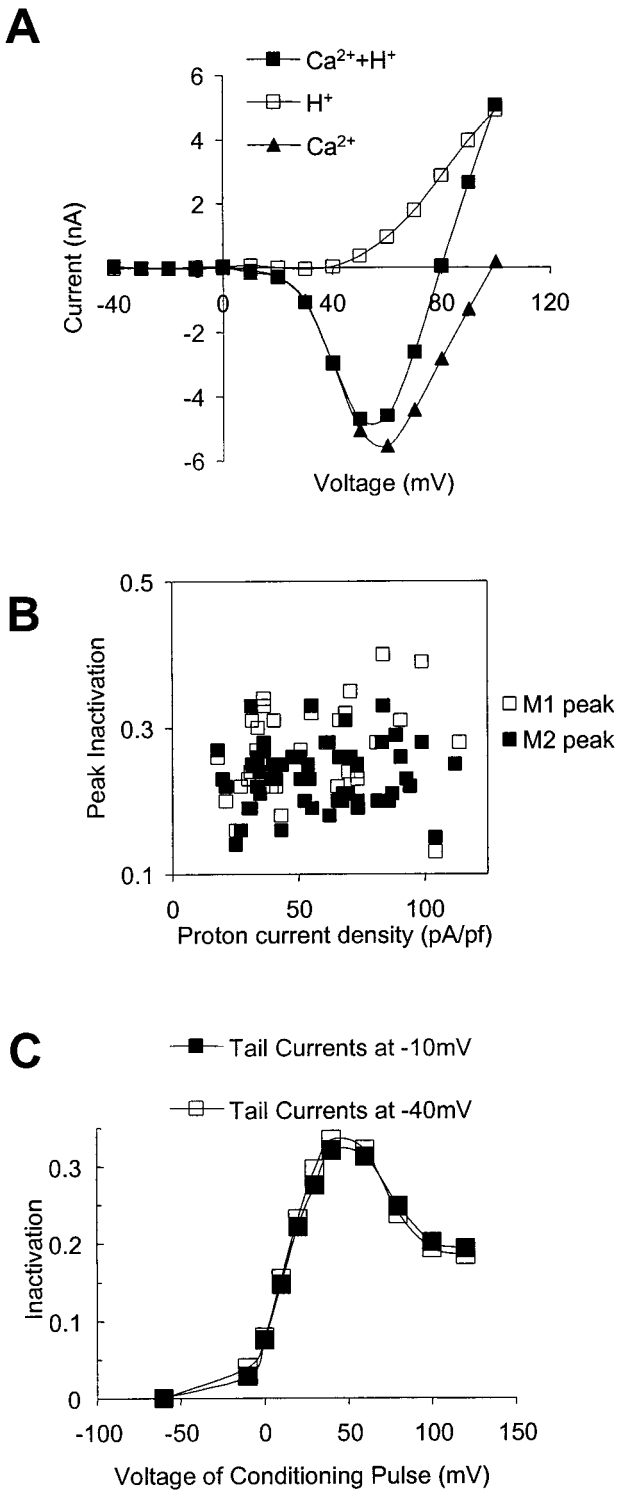

FIGURE 5 H^+ currents do not affect inactivation measurements. (*A*) Ca^{2+} currents (▲) can be obtained by subtracting currents measured in TPeA (□, H^+ currents) from those measured in standard extracellular saline (■, Ca^{2+} + H^+ currents). Currents were measured 2.5 ms after the onset of depolarization. (*B*) Peak inactivation measurements by method 1 (□; $n = 34$) and method 2 (■; $n = 55$) are not correlated with the proton current density ($R^2 < 0.001$ for both methods). Proton current density is measured as the magnitude of the outward current at +120 mV divided by the capacitance of the cell. (*C*) Inactivation measured in a cell using the standard method 2 (tail currents measured at −40 mV; □) is the same as that measured by modified method 2 (tail currents are measured at −10 mV; ■).

be carried by protons. Therefore, the tail currents measured at the end of this test pulse may be expected to have a substantial component of H^+ currents. Nevertheless, we find that H^+ current contributes very little to our measurements of the peak tail current following the test pulse. H^+ current, under our recording conditions, reverses near −10 mV. If the tail current we measure is carried in part by H^+ ions, then tail currents measured at −10 mV will have a smaller contribution of H^+ currents than those measured at −40 mV. We find, however, that whether tail currents are measured at −40 mV or −10 mV, measurements of inactivation by method 2 are identical (Fig. 5 *C*). This means that even at −40 mV, our measurements include very little H^+ tail current. We believe the absence of H^+ currents in our measurements of peak tail currents is due to the speed with which the H^+ currents deactivate below their reversal potential (Byerly et al., 1984)—the H^+ conductance may be largely deactivated by the time we measure the peak Ca^{2+} tail current (~100 μs after the end of the depolarizing pulse).

Furthermore, if the inward tail currents measured at −40 mV always had a component of inward proton tail current, then the inactivation measured by method 2 would be given by

$$\text{Measured Inactivation} = \frac{(I_{rt}^{Ca} + I^{H}) - (I_{tt}^{Ca} + I^{H})}{(I_{rt}^{Ca} + I^{H})} = \frac{I_{rt}^{Ca} - I_{tt}^{Ca}}{I_{rt}^{Ca} + I^{H}}$$

$$\leq \frac{I_{rt}^{Ca} - I_{tt}^{Ca}}{I_{rt}^{Ca}} = \text{Actual Inactivation}$$

Hence, if H^+ currents were contaminating Ca^{2+} tail current measurements, then inactivation measured by method 2 would be less than actual, and cells with larger H^+ currents would appear to have smaller levels of inactivation. However, as shown in Fig. 5 *B*, there is no correlation between H^+ current magnitude and peak levels of inactivation measured by method 2, thereby confirming that H^+ currents do not interfere with method 2 inactivation measurements.

Slow tail currents caused by large conditioning pulses do not interfere with inactivation measurements

During long positive pulses the kinetics of Ca^{2+} channel deactivation slow down; this is indicated by the appearance of prolonged tail currents after long conditioning pulses to very positive potentials. Similar phenomena have also been observed in other molluscan preparations (McFarlane, 1997). For short pulses (2.5 ms) to +140 mV, Ca^{2+} channels deactivate with a single time constant of 0.6 ms, but for longer activating pulses (500 ms) an additional slow component (τ_{slow} = 3.25 ms) of deactivation also appears (Fig. 6, *A* and *B*); the contribution of this slow component increases with the duration of positive pulse. The slow tail

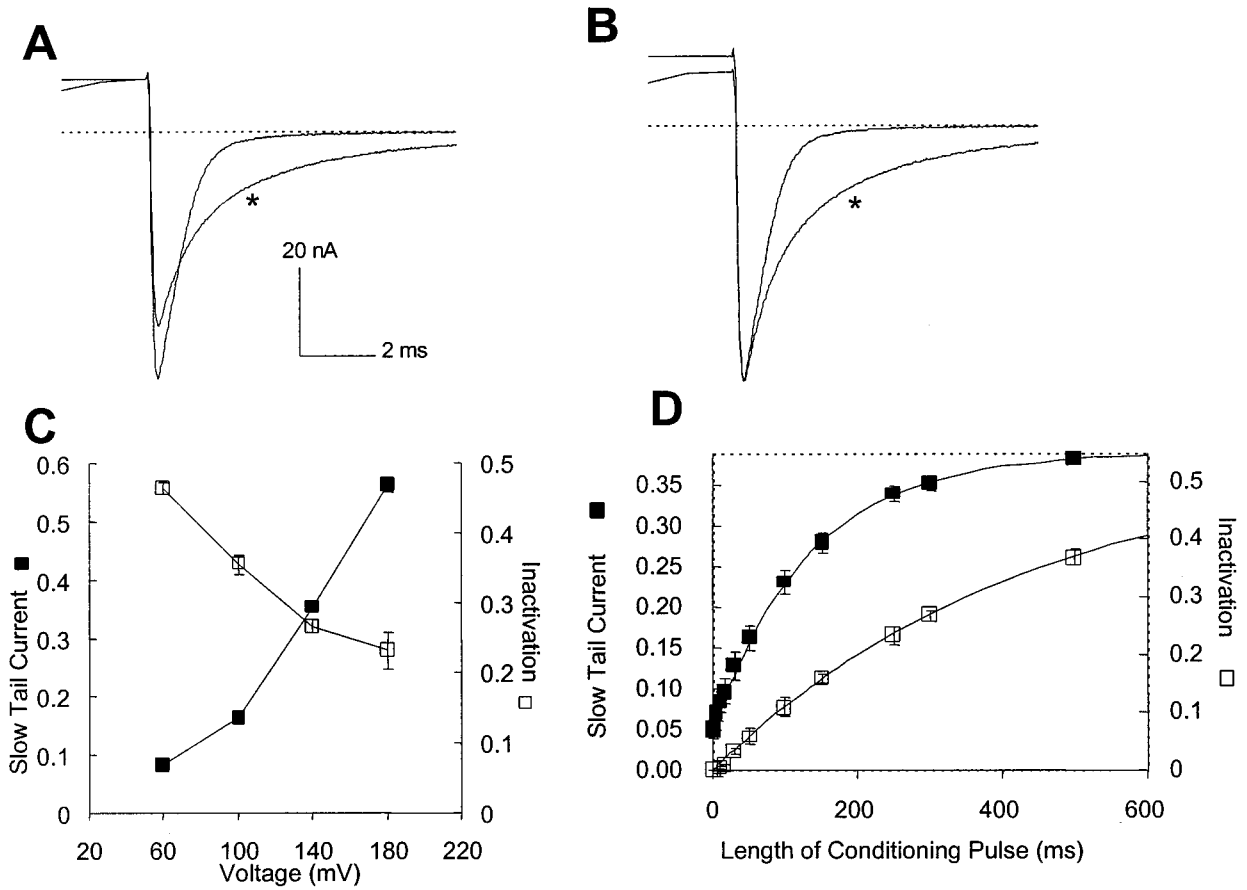

FIGURE 6 Prolonged depolarizations produce slow tail currents. (*A*) Tail currents (measured at −10 mV) after a 2.5-ms and a 500-ms pulse (*) to +140 mV. (*B*) Tail currents in *A* are scaled to the same magnitude. (*C*) Voltage dependence of the slow tail currents (■) and inactivation (□). Slow tail currents and inactivation are measured at the end of 300-ms-long pulses to different voltages. (*D*) Time course of the development of the slow tail current (■) and inactivation (□) during a conditioning pulse to +140 mV. Data points for slow tail currents and inactivation are fitted by single exponentials with time constants of 133 ms and 444 ms, respectively. The curves are scaled such that the dotted line represents the asymptote for both curves. In the protocols used in *C* and *D*, the conditioning pulses of different lengths are followed by a short test pulse to +140 or +180 mV, without an intervening gap. This is done because the gap eliminates most of the slow tail current. Tail currents are measured at −10 mV. Slow tail current is measured as the ratio of the tail current, 2 ms after the end of the depolarizing pulse, to the peak tail current; and inactivation is measured as in method 2. The measurements of inactivation here are slightly larger because of the absence of a gap before the test pulse.

currents are not due to the activation of a new conductance because they have an instantaneous *I-V* relationship expected of a Ca^{2+} current (not shown). We can also rule out a contribution from Ca^{2+}-activated Cl^- current or a Ca^{2+}-activated pump, because the slow tail currents are unaffected by a change in intracellular buffering from 5 to 0.1 mM EGTA.

Large-amplitude, long-duration positive pulses, which cause the appearance of prolonged tail currents, also cause significant differences in the amounts of inactivation measured using the two methods. These slow tail currents have been proposed to signify a second open state of the channel (McFarlane, 1997), but in that case, the relationship between the inactivated state and the second open state is unclear. Therefore, we investigated how inactivation is related to the appearance of slow tail currents. For conditioning pulses between +60 mV and +180 mV, inactivation decreases, whereas the slow component of the tail current increases, with the conditioning pulse voltage (Fig. 6 *C*). Increasing the duration of the conditioning pulse increases both the inactivation and the slow component of the tail current; however, the time constants for the two processes are different. At the end of a 500-ms-long pulse to +140 mV, the slow tail current has already reached its steady-state value while inactivation is still increasing (Fig. 6 *D*). Thus the appearance of slow tail currents has a voltage and time dependence different from those of inactivation. This rules out the simple model in which the slow tail currents could be explained by channels recovering from inactivation at negative potentials, but leaves open the possibility that the inactivated state could be linked to a second open state in some more complex way (see model 2 in the Discussion).

In both methods large conditioning pulses to very positive voltages result in prolonged tail currents that can take up to 15 ms to completely turn off. If a short test pulse is applied before complete deactivation of the Ca^{2+} channel currents, then the tail currents following the short test pulse also have a component with a slow time course. However,

once the tail currents have completely deactivated, short test pulses do not elicit prolonged tail currents. For this reason, in the two protocols used in this study, the test pulses follow the conditioning pulses after a gap of 17.5 or 20 ms. Thus, in method 2, we avoid the problem of comparing fast reference tail currents with slow tail currents elicited by a test pulse following a conditioning pulse to very positive potentials.

DISCUSSION

In this study, two methods have been employed to measure the inactivation of Ca^{2+} channels: method 1 uses currents elicited during a pulse to +40 mV, and method 2 uses tail currents following a short depolarization to +120 mV to measure the Ca^{2+} conductance of the cells. We find that there is a consistent difference between these two measurements that cannot be explained as an error due to contamination by H^+ currents or slow tails elicited by conditioning pulses. This difference is due to the different test pulse voltages applied in the two cases.

Both methods yield bell-shaped inactivation curves. Such bell-shaped inactivation curves have often been associated with the presence of Ca^{2+}-dependent inactivation. However, studies conducted in our laboratory have shown that the large amount of intracellular Ca^{2+} buffer used in the experiments described here (5 mM EGTA) completely suppresses all Ca^{2+}-dependent inactivation (Gera and Byerly, 1998). Inactivation measurements under these conditions are insensitive to changes in Ca^{2+} influx and to substitution of external Ca^{2+} with Ba^{2+}. Increasing the intracellular Ca^{2+} buffering from 5 mM EGTA to 11 mM 1,2-bis(2-aminophenoxy)ethane-*N,N,N,N*-tetraacetic acid (BAPTA) also does not affect the inactivation, although decreasing it to 0.1 mM EGTA causes an additional Ca^{2+}-dependent component of inactivation to appear. Hence the inactivation measured in this study occurs through voltage-dependent mechanisms. Previous studies of native Ca^{2+} channels in bullfrog sympathetic neurons (Jones and Marks, 1989) and of recombinant Ca^{2+} channels transfected into HEK 293 cells (Patil et al., 1998) have also found that purely voltage-dependent mechanisms can yield bell-shaped inactivation curves.

Test pulse dependence of inactivation measurements

We find that the measurement of inactivation is inherently dependent upon the test pulse potential used. Inactivation curves measured using test pulses to less positive voltages (such as +40 mV) have a more pronounced bell shape than those obtained using test pulses to very positive potentials (such as +120 mV). We have considered two models that can account for this behavior of Ca^{2+} channels: a two-channel model and a single-channel model.

The two-channel model

The different magnitudes of inactivation measured by methods 1 and 2 can be explained by assuming that we are recording Ca^{2+} current from two types of Ca^{2+} channels in *Lymnaea* neurons and that these two classes of Ca^{2+} channels have different inactivation properties. One class of Ca^{2+} channels (type I) is activated at lower voltages, and the other class (type II) is activated at higher voltages. Because the test pulse in method 2 to +120 mV maximally activates both types of Ca^{2+} channels, the inactivation measured by this method represents the inactivation of all Ca^{2+} channels. On the other hand, the test pulse in method 1 (to a lower voltage of +40 mV) activates a larger proportion of type I channels than type II channels; consequently, the inactivation measured with method 1 is influenced more by the inactivation of type I channels. This model is illustrated in Fig. 7. The activation curve, obtained experimentally from tail currents following brief pulses to activating voltages, can be fitted by a single Boltzmann function or by a sum of two or more Boltzmann functions. For the purposes of this model, we express the activation curve as a sum of two Boltzmann functions, each of which represents the activation of the one type of Ca^{2+} channel (Fig. 7 *A*). The measured inactivation is a weighted average of the inactivation of the two types of Ca^{2+} channels, the weights being the relative number of channels of each type that are activated by the test pulse voltage. Therefore, inactivation measured using a test potential *tp* is given by

$$\text{Inactivation}_{tp} = I_A \cdot a_{tp} + I_B \cdot b_{tp}, \quad (1)$$

where a_{tp}, b_{tp} are the proportions of the reference pulse current carried by type I and type II channels at test potential *tp*, and I_A, I_B are the inactivated fractions of the type I and type II channels, respectively. Data obtained using methods 1 and 2 provide us with the measurements of inactivation for test pulses to +40 mV and +120 mV; also, *a* and *b* for these test potentials were estimated from the Boltzmanns in Fig. 7 *A*. Thus we have two equations (corresponding to the inactivation measured at test potentials of +40 mV and +120 mV) in two unknowns (I_A and I_B) for every conditioning pulse voltage. Hence we can determine I_A and I_B for different conditioning voltages and obtain the inactivation curves for the two types of channels, as shown in Fig. 7 *B*. The inactivation curve of type I channels is more bell shaped than that of type II channels, corresponding to the observation that test pulses to lower voltages result in inactivation curves that are more bell shaped. Inactivation predicted by this model for test pulses to +30, +50, and +120 mV is shown in Fig. 7 *C* and is similar to the measured inactivation shown in Fig. 4 *A*.

Although this model is attractive in its simplicity, we do not have any other evidence for the presence of two or more types of Ca^{2+} channels in *Lymnaea* neurons. Hayden and Man-Son-Hing (1988) have reported the presence of HVA and LVA channels in the neurons of *Heliosoma*, a mollusc closely related to *Lymnaea*; however, similar analyses in

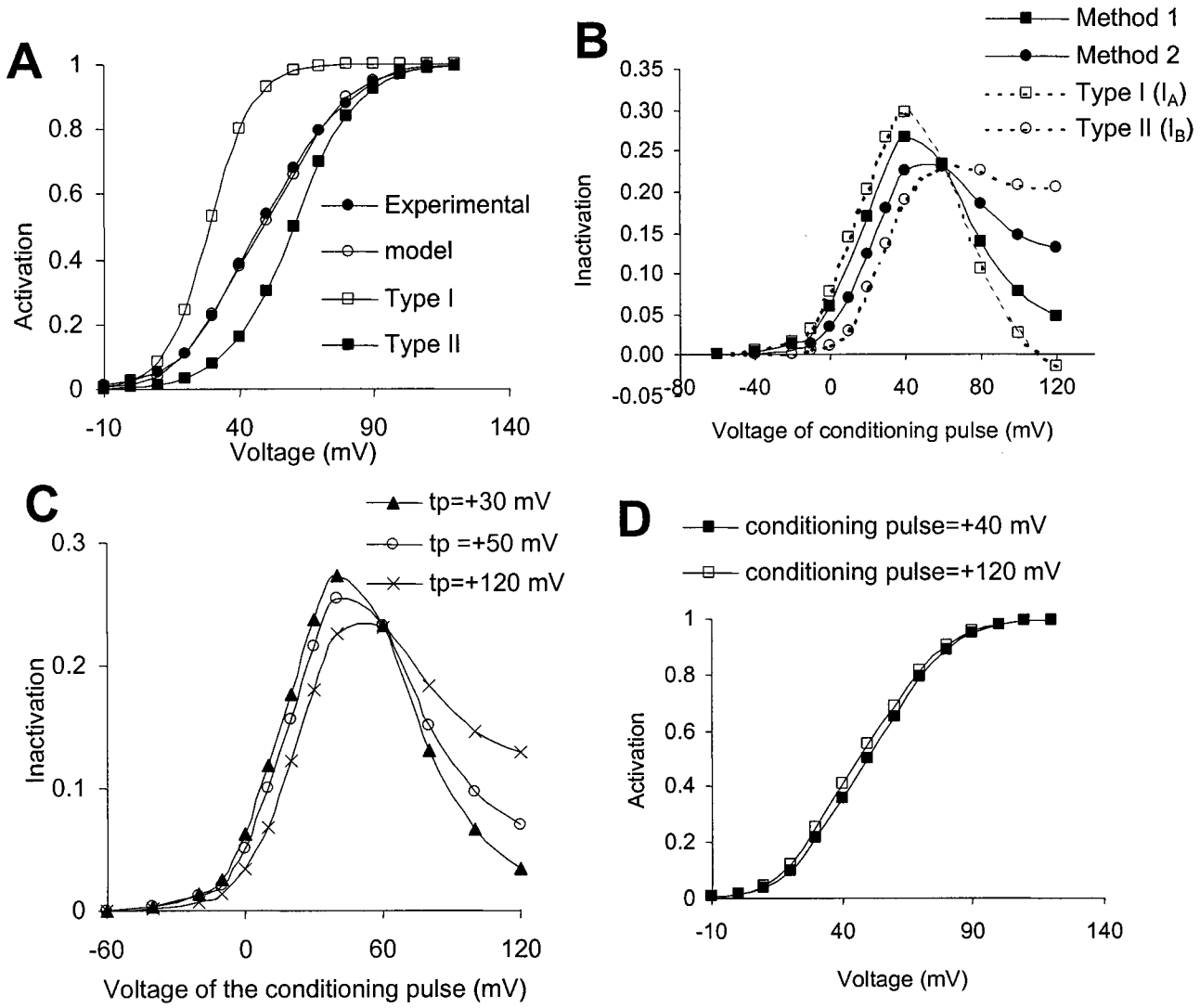

FIGURE 7 The two-channel model. (*A*) The experimental activation curve (●, $n \geq 33$) is obtained by normalizing the tail currents measured at the end of 20-ms pulses to various potentials to that after a pulse to +120 mV. The model assumes that two Boltzmann functions with $V_{1/2}$ of +29 and +60 mV and slope factors of 8 and 12 mV represent the activation of type I (□) and type II (■) channels, respectively. These parameters are not uniquely defined and were chosen for this model because they yield a large difference between the half-activation voltages ($V_{1/2}$) of the two channel types. Type I channels represent 34% of the total number of channels, and the activation curve for the total Ca^{2+} current predicted by the model (○) closely matches that obtained experimentally (●). (*B*) Inactivation curves for type I (□) and type II (○) channels are computed from those obtained using method 1 (■, $n \geq 33$) and method 2 (●, $n \geq 53$). The inactivation curve for method 1 has been adjusted to eliminate errors due to residual inactivation caused by the reference pulse. (*C*) Inactivation predicted by the model for test pulse potentials of +30 mV (▲), +50 mV (○), and +120 mV (×). (*D*) Activation curves predicted by the model after a 150-ms conditioning pulse to 40 mV (■) and to +120 mV (□).

Lymnaea neurons have failed to resolve more than one type of Ca^{2+} channel. As mentioned earlier, the activation curve for Ca^{2+} currents in *Lymnaea* neurons (shown in Fig. 7 *A*) is well described with a single Boltzmann function. Single-channel studies have proved inconclusive, because most Ca^{2+} channels appear in clusters and single-channel conductances cannot be readily resolved (unpublished observations). *Lymnaea* Ca^{2+} channel tail currents elicited by short, low-potential activating pulses do not exhibit a slow component, which is considered an indicator of LVA channels in vertebrate neurons. None of the divalent metals (including Cd^{2+} and Ni^{2+}) distinguish more than one type of *Lymnaea* Ca^{2+} channel. These Ca^{2+} channels have not been identified with any vertebrate HVA Ca^{2+} channel type (L, N, or P/Q type) or divided into classes by selective pharmacological agents. They are insensitive to both ω-conotoxin GVIA and dihydropyridines (unpublished observations). Although these observations do not preclude the possibility of two or more types of Ca^{2+} channels being present in these neurons, they also do not provide any support for this idea.

It is possible that the two types of channels hypothesized in the model may not be two entirely different Ca^{2+} channel proteins, but merely functional modifications of the same protein. Thus the two classes of Ca^{2+} channels may represent phosphorylated and unphosphorylated, or G-protein-

bound and G-protein-free states of a single class of Ca^{2+} channels, which have different activation and inactivation properties.

Single-channel model

Because it is possible that only one type of Ca^{2+} channel is present in these neurons, we have looked for another model that does not require distinct classes of Ca^{2+} channels to explain the test pulse dependence of inactivation measurements. Three-state models of Ca^{2+} channels (with only one closed, one open, and one inactivated state) cannot generate this behavior. Because earlier work on molluscan Ca^{2+} channels has suggested the presence of two open states (McFarlane, 1997), we have developed a model around this possibility. Our model has two open states, O and O*, two corresponding closed states, C and C*, and an inactivated state, I, reached via the open state O* (Fig. 8 *A*).

In this model, channels in state C open at lower voltages, whereas those in C* require higher voltages to open. A test pulse to +120 mV drives channels in both closed states (C and C*) to their respective open states. These transitions correspond to the opening of type I and type II channels of the previous model, with the one important distinction that in this model, channels can go from one open state to the other (with rate constants α' from O to O*, and β' from O* to O). As the potential increases, transitions from O to O* are favored; α' increases, whereas β' decreases with voltage. However, the net flux of channels from O to O* is maximum during conditioning pulses to moderately positive voltages; at very high voltages, the high occupancy of O* decreases the net flux of channels from O to O*. The forward rate constant to the inactivated state, α_I, decreases with voltage, whereas the reverse rate constant, β_I, increases with voltage. Therefore the probability of channels in O* entering the inactivated state I is higher at intermediate voltages. The voltage dependence of α_I and β_I in this model is similar to that of the corresponding rate constants in a model proposed by Jones and Marks (1989).

The parameters in the model (Table 1) have been chosen so that at the holding potential (−60 mV) at steady state, the channels are equally distributed into the two closed states, C and C*, with almost none in the inactivated state, I. After a conditioning pulse has been applied and the membrane is at the holding potential again (i.e., during the gap), some channels are left in the inactivated state, while the others are redistributed between the closed states, C and C*, although not in the same proportion as at rest. If we consider only the channels in the closed state C, before and after the application of the conditioning pulse we can define "apparent C inactivation" or I_C as

$$I_C = \frac{f_C^{rest} - f_C^{cp}}{f_C^{rest}}, \tag{2}$$

where f_C^{rest} and f_C^{cp} are the fractions of channels in state C, at rest and after the conditioning pulse, respectively. During a conditioning pulse, channels can transition between open states, but upon repolarization the majority of channels in O close into C, and those in O* close into C* (at −60 mV, α' and β' are much smaller than the deactivation rate constants). Hence the difference in the number of channels in C before and after a conditioning pulse is due to the number of channels that have left O and entered O*. Therefore,

$$I_C = \frac{f_{O\rightarrow O^*}}{f_C^{rest}},$$

where $f_{O\rightarrow O^*}$ is the net flux of channels from state O to O* during the conditioning pulse. Similarly, for channels in state C*, we can define "apparent C* inactivation" or I_{C^*} as

$$I_{C^*} = \frac{f_{C^*}^{rest} - f_{C^*}^{cp}}{f_{C^*}^{rest}} = \frac{f_I - f_{O\rightarrow O^*}}{f_{C^*}^{rest}}, \tag{3}$$

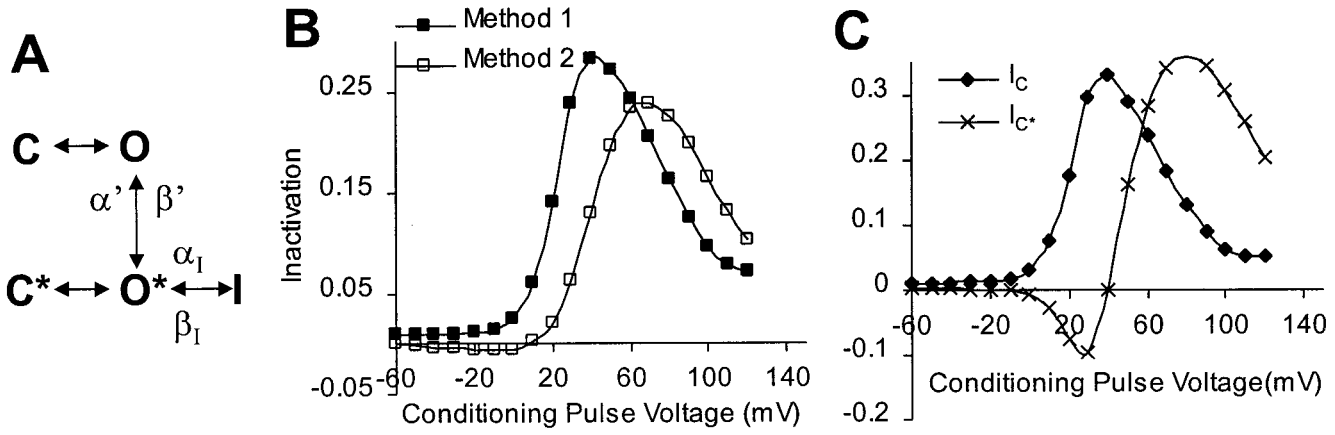

FIGURE 8 The single-channel model. (*A*) A schematic representation of the model. (*B*) The inactivation curves predicted by the model for method 1 (■) and method 2 (□). The model assumes that half of the channels at rest are in the closed state C and half in C*. (*C*) The apparent inactivation curves, I_C (♦) and I_C* (×), as defined in the model (Eqs. 2 and 3).

TABLE 1 Parameters for the rate constants used in the single-channel model

	α_O	β_O	α_{O*}	β_{O*}	α'	β'	α_I	β_I
A_{max} (ms^{-1})	1.5	7.5	1	1	0.022	0.22	0.07	0.049
f (mV^{-1})	0.06	−0.07	0.1	−0.1	0.04	−0.01	−0.025	0.02
$V_{1/2}$ (mV)	30	0	60	70	30	−100	20	150

Each rate constant is expressed as a function of the voltage V, given by $A_{max}/1 + \exp[-f \cdot (V - V_{1/2})]$. α_O and α_{O*} are the forward rate constants, whereas β_O and β_{O*} are the reverse rate constants from the closed states C and C* to the open states O and O*, respectively.

where f_{C*}^{rest}, f_{C*}^{cp}, and f_I are fractions of channels in state C*, before and after the conditioning pulse, and in state I after the conditioning pulse, respectively.

The inactivation measured in this model using a test pulse to any potential *tp* is a weighted average of these two apparent inactivations and is given by

$$\text{Inactivation}_{tp} = I_C \cdot a_{tp} + I_{C*} \cdot b_{tp}, \quad (4)$$

where a_{tp}, b_{tp} are the fractions of the reference pulse current carried by channels in the open states O and O*, respectively, for a test pulse potential, *tp*. Equation 4 is analogous to Eq. 1 of the previous model, and the test pulse dependence of inactivation measurements is explained using a similar rationale. Different proportions of reference pulse current are carried by the two open states for different test potentials, leading to different measurements of inactivation. When the test pulse is to +120 mV, almost all channels initially in the closed states C and C* are activated, i.e., $a_{tp} = f_C^{rest}$ and $b_{tp} = f_{C*}^{rest}$. Therefore,

$$\text{Inactivation}_{120mV} = I_C \cdot f_C^{rest} + I_{C*} \cdot f_{C*}^{rest}$$
$$= f_{O\rightarrow O*} + (f_I - f_{O\rightarrow O*}) = f_I.$$

Hence the inactivation measured by a test pulse to +120 mV is an accurate estimate of the fraction of channels in the inactivated state. However, when the test pulse is to lower voltages, parameter *a* becomes larger relative to parameter *b* (i.e., a larger fraction of the reference pulse current is carried through channels in the open state O), and consequently, the measured inactivation is dominated by I_C. However, I_C only reflects the net number of channels making the transition from O to O*, not the fraction in state I. As explained earlier, the net flux of channels from O to O* is maximum at moderately positive voltages, which makes I_C bell shaped. Thus, as the test pulse becomes less positive, measured inactivation becomes more bell shaped and peaks at lower voltages.

Fig. 8 *B* shows the inactivation curves predicted by this model for a test pulse to +40 mV and to +120 mV, and Fig. 8 *C* gives the corresponding apparent inactivation curves, I_C and I_{C*}. Note that I_{C*} is negative for small positive voltages, because more channels make the transition from O to O* than make the transition from O* to I at these voltages. It should be noted, however, that although the presence of a second slower component of the deactivating tail currents was a primary motivation for such a model with multiple open states, this model cannot reproduce the dependence of tail current kinetics upon the length and voltage of the depolarizing pulse.

CONCLUDING REMARKS

Dependence of inactivation measurements on test pulse potential may be a property common to many Ca^{2+} channels. Although we are aware of only one previous report of test pulse dependence of inactivation measurements (Akaike et al., 1978), we suspect that this may be a general phenomenon that has been overlooked in earlier studies of inactivation. Standard models of inactivation predict that a conditioning pulse inhibits a fixed proportion of current elicited by test pulses to all voltages. Hence, activation curves measured after a conditioning pulse should only be scaled-down versions of those measured without a conditioning pulse. However, test pulse dependence of inactivation measurements implies that a conditioning pulse suppresses currents for some test pulse voltages more than for others and hence would also cause a change in the shape of the activation curve. This would be seen as either a voltage shift or a change in the slope factor of the activation curve. Both of our models of inactivation predict that a 150-ms-long pulse to +40 mV causes a slight shift in the activation curve to the right, whereas a 150-ms-long pulse to +120 mV shifts the activation curve to the left (as shown for the two-channel model in Fig. 7 *D*). The shifts predicted by the model in this case are too small to be experimentally detected. However, such shifts of activation curves toward negative voltages by long, very positive prepulses have been described earlier for Ca^{2+} channels in other preparations (Bean, 1989; Sculptoreanu et al., 1993; Fleig and Penner, 1996). It would follow, therefore, that measurements of inactivation in these Ca^{2+} channels will also be dependent upon test pulse potentials, especially after very positive conditioning pulses.

Our models suggest that very positive test pulses are required to accurately measure the fraction of total channels that are inactivated. However, for physiological relevance, it may be more desirable to understand the behavior of channels at small positive test potentials. Our results show that both methods I and II give valid measurements of inactivation, as long as their results are interpreted within the context of the test pulse potential used.

We thank Dr. John P. Walsh and Dr. Barry D. Johnson for helpful comments on an early version of the manuscript.

This work was supported by National Institutes of Health grant NS 28484.

REFERENCES

Akaike, N., K. S. Lee, and A. M. Brown. 1978. The calcium current of *Helix. J. Gen. Physiol.* 71:509–531.

Bean, B. P. 1989. Neurotransmitter inhibition of neuronal calcium channel currents by changes in channel voltage dependence. *Nature.* 340: 153–156.

Byerly, L., and S. Hagiwara. 1982. Calcium currents in internally perfused nerve cell bodies of *Limnea stagnalis. J. Physiol. (Lond.).* 322:503–528.

Byerly, L., R. Meech, and W. Moody, Jr. 1984. Rapidly activating hydrogen ion currents in perfused neurones of the snail, *Lymnaea stagnalis. J. Physiol. (Lond.).* 351:199–216.

Eckert, R., and D. Tillotson. 1981. Calcium-mediated inactivation of the calcium conductance in caesium-loaded giant neurones of *Aplysia californica. J. Physiol. (Lond.).* 314:265–280.

Fleig, A., and R. Penner. 1996. Silent calcium channels generate excessive tail currents and facilitation of calcium currents in rat skeletal myoballs. *J. Physiol. (Lond.).* 494.1:141–153.

Gera, S., and L. Byerly. 1998. Cytochalasin B and TFP greatly enhance calcium channel inactivation. *Biophys. J.* 72:A140 (Abstr.).

Hagiwara, S., and H. Ohmori. 1982. Studies of calcium channels in rat clonal pituitary cells with patch electrode voltage clamp. *J. Physiol. (Lond.).* 331:231–252.

Hayden, P. G., and H. Man-Son-Hing. 1988. Low- and high-voltage-activated calcium currents: their relationship to the site of neurotransmitter release in an identified neuron of Heliosoma. *Neuron.* 1:919–927.

Isom, L. L., K. S. De Jongh, and W. A. Catterall. 1994. Auxiliary subunits of voltage-gated ion channels. *Neuron.* 12:1183–1194.

Johnson, B. D., and L. Byerly. 1993. Photo-released intracellular Ca^{2+} rapidly blocks Ba^{2+} current in *Lymnaea* neurons. *J. Physiol. (Lond.).* 462:321–347.

Johnson, B. D., and L. Byerly. 1994. Ca^{2+} channel Ca^{2+}-dependent inactivation in a mammalian central neuron involves the cytoskeleton. *Pflügers Arch.* 429:14–21.

Jones, S. W., and T. N. Marks. 1989. Calcium currents in bullfrog sympathetic neurons. II. Inactivation. *J. Gen. Physiol.* 94:169–182.

McFarlane, M. B. 1997. Depolarization-induced slowing of Ca^{2+} channel deactivation in squid neurons. *Biophys. J.* 72:1607–1621.

Neher, E. 1995. Voltage offsets in patch-clamp experiments. *In* Single-Channel Recording, 2nd Ed. B. Sakmann and E. Neher, editors. Plenum Press, New York. 147–153.

Olcese, R., N. Qin, T. Schneider, A. Neely, X. Wei, E. Stefani, and L. Birnbaumer. 1994. The amino terminus of a calcium channel β subunit sets rates of channel inactivation independently of the subunits effect on activation. *Neuron.* 13:1433–1438.

Patil, P. G., D. L. Brody, and D. T. Yue. 1998. Preferential closed-state inactivation of neuronal calcium channels. *Neuron.* 20:1027–1038.

Schuhmann, K., C. Romanin, W. Baumgartner, and K. Groschner. 1997. Intracellular Ca^{2+} inhibits smooth muscle L-type Ca^{2+} channels by activation of protein phosphatase type 2B and by direct interaction with the channel. *J. Gen. Physiol.* 110:503–513.

Sculptoreanu, A., T. Scheur, and W. A. Catterall. 1993. Voltage dependent potentiation of L type Ca^{2+} channels due to phosphorylation by cAMP-dependent protein kinase. *Nature.* 364:240–243.

Thomas, R. C., and R. W. Meech. 1982. Hydrogen ion currents and intracellular pH in depolarized voltage clamped snail neurones. *Nature.* 299:826–828.

Tillotson, D. 1979. Inactivation of Ca conductance dependent on entry of Ca ions in molluscan neurons. *Proc. Natl. Acad. Sci. USA.* 76: 1497–1500.